THE JOURNAL OF BIOLOGICAL CHEMISTRY VOL. 281, NO. 51, pp. 39642–39648, December 22, 2006

Seeing the Process of Histidine Phosphorylation in Human Bisphosphoglycerate Mutase*[S]

Received for publication, July 6, 2006, and in revised form, October 10, 2006 Published, JBC Papers in Press, October 18, 2006, DOI 10.1074/jbc.M606421200

Yanli Wang[‡], Lin Liu[‡§], Zhiyi Wei[‡§], Zhongjun Cheng[‡§], Yajing Lin[‡], and Weimin Gong[‡§1]

From the [‡]National Laboratory of Biomacromolecules, Institute of Biophysics, Chinese Academy of Sciences, Beijing 100101, China and [§]School of Life Sciences, University of Science and Technology of China, Hefei, Anhui 230026, China

Bisphosphoglycerate mutase is an erythrocyte-specific enzyme catalyzing a series of intermolecular phosphoryl group transfer reactions. Its main function is to synthesize 2,3-bisphosphoglycerate, the allosteric effector of hemoglobin. In this paper, we directly observed real-time motion of the enzyme active site and the substrate during phosphoryl transfer. A series of high resolution crystal structures of human bisphosphoglycerate mutase co-crystallized with 2,3-bisphosphoglycerate, representing different time points in the phosphoryl transfer reaction, were solved. These structures not only clarify the argument concerning the substrate binding mode for this enzyme family but also depict the entire process of the key histidine phosphorylation as a "slow movie". It was observed that the enzyme conformation continuously changed during the different states of the reaction. These results provide direct evidence for an "in line" phosphoryl transfer mechanism, and the roles of some key residues in the phosphoryl transfer process are identified.

Phosphoryl transfer is an important biochemical reaction involved in numerous critical physiological processes in life. It is thought that the catalyzed reaction occurs by nucleophilic attack on the reaction center phosphorus, for which an "in line" mechanism is believed to be the most likely (1), although an adjacent mechanism has been suggested to be a possibility in some cases (2). The in line mechanism describes a continuum between two extremes, associative and dissociative mechanisms.

Bisphosphoglycerate mutase (BPGM)[2] and cofactor-dependent phosphoglycerate mutase (dPGM) are tri-functional enzymes, catalyzing a series of intermolecular phosphoryl group transfer reactions (3, 4). Both BPGM and dPGM can catalyze the same three overall reactions for which phosphorylation of the catalytic histidine by 2,3-bisphosphoglycerate is the first step. Previous studies of BPGM and dPGMs have provided important but so far incomplete information on the structural basis for the specific activities and molecular mechanisms (5–14). Although a number of structures of dPGMs (9, 10, 12, 13, 15–18) and human BPGM (8) have been reported, no structure of the enzyme·substrate complex is available. The structure of the dPGM from *Escherichia coli* in complex with its vanadate inhibitor modeled the monophosphoglycerate and bisphosphoglycerate binding (9). However, this model is inconsistent with the *Saccharomyces cerevisiae* dPGM/3-PGA complex structure, although the electron density for the 3-PGA in this structure is very poor (19). Thus the model of substrate binding and the roles of active site residues as well as the possible conformational changes during the catalysis have remained a mystery.

Here we present the crystal structures of human BPGM binding with 2,3-BPG, 3PGA + AlF_4^-, or 3-PGA as well as the equilibrated structures of phosphorylated BPGM and BPGM binding with 2,3-BPG. We observed that the process of histidine phosphorylation in human BPGM was dramatically slowed down under crystallization conditions so that each step of the reaction had been captured. The series of structures reveal the stepwise conformational changes of the enzyme during the reaction. The nucleophile histidine moved back and forth to access the substrate and catch the phosphoryl group, whereas the substrate remained relatively still.

EXPERIMENTAL PROCEDURES

The expression and purification of human BPGM were performed as described previously (8). All crystals were grown using the hanging drop vapor diffusion method. Three conditions were used to obtain BPGM·substrate complex crystals. Condition A: protein sample (30 mg/ml) was mixed with 2,3-BPG at a 1:20 molar ratio; the reservoir solution was 22–24% (w/v) polyethylene glycol 6000, 0.1 M Hepes, pH 7.0, at 4 °C. Condition B: as for condition A but with a pH value of 8.0 and at 16 °C. Condition C: protein sample (30 mg/ml) was mixed with NaF, $AlCl_3$, and 3-PGA at a 1:30:10:10 molar ratio. All crystals were flash frozen in liquid nitrogen without any cryoprotectant. The diffraction data were collected at the Beijing Synchrotron Radiation Facility equipped with a Mar CCD detector, flash cooled with liquid nitrogen at 100 K. Diffraction data were pro-

* This work is supported by National Funding for outstanding young scientists (Grant No. 30225015), the 973 Program of the Ministry of Science and Technology (Grant No. 2004CB720008), the National Natural Science Foundation of China (Grant Nos. 10490913 and 30500100), and the Chinese Academy of Sciences (KSCX1-YW-R-61). The costs of publication of this article were defrayed in part by the payment of page charges. This article must therefore be hereby marked "*advertisement*" in accordance with 18 U.S.C. Section 1734 solely to indicate this fact.

[S] The on-line version of this article (available at http://www.jbc.org) contains supplemental Figs. 1–3.

The atomic coordinates and structure factors (code 2H4Z, 2HHJ, 1H4X, 2A9J, and 2F90) have been deposited in the Protein Data Bank, Research Collaboratory for Structural Bioinformatics, Rutgers University, New Brunswick, NJ (http://www.rcsb.org/).

[1] To whom correspondence should be addressed: Institute of Biophysics, 15 Datun Rd., Chaoyang Dist., Beijing 100101, China. Tel.: 86-10-64888467; Fax: 86-10-64888513; E-mail: wgong@ibp.ac.cn.

[2] The abbreviations used are: BPGM, bisphosphoglycerate mutase; BPG, bisphosphoglycerate; dPGM, cofactor-dependent phosphoglycerate mutase; PGA, phosphoglycerate.

TABLE 1
Statistics of data collection and structure refinement
Numbers in parentheses represent the values for the highest resolution shell.

Data set	Structure 1	Structure 2	Structure 3	Structure 4	Structure 5
Data collection					
Resolution (Å)	100-2.0 (2.05-2.0)	30.0-1.5 (1.53-1.50)	50-1.85 (1.89-1.85)	30-2.0 (2.05-2.0)	50-2.0 (2.05-2.0)
Space group	$P2_12_12_1$	$P2_12_12_1$	$P2_12_12_1$	$P2_12_12_1$	$P2_12_12_1$
a (Å)	49.1	48.7	48.5	48.7	48.4
b (Å)	71.2	71.6	71.4	71.4	71.7
c (Å)	159.3	159.2	160.2	159.8	158.8
Completeness (%)	96.7 (95.8)	97.8 (92.3)	98.0 (94.2)	96.4 (96.6)	98.4 (98.2)
Observed reflections	381,231	1,004,338	930,645	522,915	667,830
Unique reflections	37,662	88,158	47,571	37,400	37,619
I/σ	17.2 (3.6)	19.6 (1.8)	21.3 (4.4)	45.3 (17.7)	33.0 (6.2)
R_{merge} (%)	0.066 (0.326)	0.069 (0.438)	0.081 (0.284)	0.038 (0.070)	0.075 (0.298)
Refinement					
R-factor	0.184 (0.239)	0.182 (0.241)	0.180 (0.242)	0.200 (0.221)	0.183 (0.203)
R_{free}	0.225 (0.281)	0.209 (0.247)	0.215 (0.275)	0.236 (0.257)	0.228 (0.248)
Number of non-hydrogen atoms					
Protein	4113	4158	4140	4056	4150
Water	555	761	698	456	612
Ligand	30	30	22	22	32
r.m.s.d.[a] from ideal					
Bond length (Å)	0.005	0.004	0.005	0.005	0.005
Bond angles (°)	1.3	1.2	1.2	1.2	1.2
Average *B*-factor (Å^2)					
Protein	24.1	15.9	19.5	24.3	20.3
Ligand	25.3	14.5	16.2	23.5	16.2
Water	33.2	29.6	32.6	33.5	31.6

[a] Root mean square deviation.

cessed with DENZO and SCALEPACK programs (20). The crystals belonged to space group $P2_12_12_1$ with similar unit cell parameters. There was a dimer in the asymmetric unit. The mode of dimerization was the same as in free BPGM, indicating that the dimer was a physiological one. The crystal structures were determined by molecular replacement using the free BPGM structure (Protein Data Bank code 1T8P) as the search model and were refined with the non-crystallography symmetry restraint using the crystallography NMR software package (21) and program O (22). Substrate and water molecules were included at the later steps of refinement. The quality and stereochemistry of the final models were analyzed with PROCHECK (23). In the Ramachandran plots of all structures, more than 91.8% of the residues are located in the most-favored regions, and only Ser-24 is located in the general allowed region as in the free BPGM structure (8). The statistics of data collection and structure refinement are listed in Table 1.

RESULTS

Structure of BPGM Bound with a 2,3-BPG before Reaction—To obtain the BPGM·substrate complex structure, we co-crystallized human BPGM with 2,3-BPG at 4 °C and at room temperature (crystallization condition A). In the crystal grown at 4 °C, the electron density clearly shows the presence of a 2,3-BPG molecule (Fig. 1*A*, *structure 1*). The Nϵ-2 atom of the catalytic His-11 formed a hydrogen bond with the 2′-phosphoryl group, which was also stabilized by the side chains of Arg-10, Arg-62, His-188, the amide atom of Gly-189, and four water molecules. On the other side, the 3′-phosphoryl group was anchored by hydrogen bonds with Arg-100, Arg-116, Arg-117, Tyr-92, Asn-190, and two water molecules. The carboxylate group of C-1 atom hydrogen bonds to the amide atoms Ser-24 (Fig. 5*C* and Supplemental Fig. 1). Compared with free BPGM (8), residues 99–122 move toward the active site, with a 36° rotation toward the "core" domain (calculated by the program DynDom (24)), putting Arg-100, Arg-116, and Arg-117 into the active site. The C-terminal residues 236–250 also shift along the C-terminal helix by more than 3 Å. Residues 251–256, which were disordered in free BPGM, stretched forward with clear electron density. Thus the active pocket is fully closed. In addition, the backbone conformations of residues 12–21 also significantly changed to accommodate 2,3-BPG binding (Fig. 2).

Equilibrated Structures of BPGM Bound with 2,3-BPG and Phosphorylated BPGM—Unexpectedly, when BPGM was co-crystallized with 2,3-BPG at room temperature (crystallization condition B) for 15 days, continuous electron density was observed between His-11 and 2,3-BPG (Fig. 1*B*). Structure refinement was carefully carried out to 1.5-Å resolution. This density was defined as a mixture of a 2,3-BPG, ready for reaction and a phosphoryl group covalent bonding to His-11 plus a 3-PGA (Fig. 3). The two monomers in the asymmetric unit exhibited the same structure with slightly different occupancies of the ligands (40% of His-11 phosphorylated with 60% of 2,3-BPG unreacted in monomer A and 65% of His-11 phosphorylated with 35% of 2,3-BPG unreacted in monomer B) (Figs. 4 and 5*D*). The phosphorylated histidine is the intermediate in the BPGM reaction. In this mixed structure, each of the active site residues exhibits a single conformation indicating that this is an equilibrated state in which the phosphoryl group is being transferred. An equilibrated mixture of states in the enzyme reaction was also observed for 3-hydroxy-3-methylglutaryl-CoA synthase (25, 26). For the phosphorylated BPGM, the covalent N-P bond length of phosphorylated His-11 is 1.7 Å, consistent with the calculated value of 1.76 Å (27). Compared with structure 1 (Fig. 1*A*), further conformational changes occurred at residues 11–19 with the Cα atoms shifting an average of 1 Å, making the imidazole ring of His-11 rotate about 20° and move toward

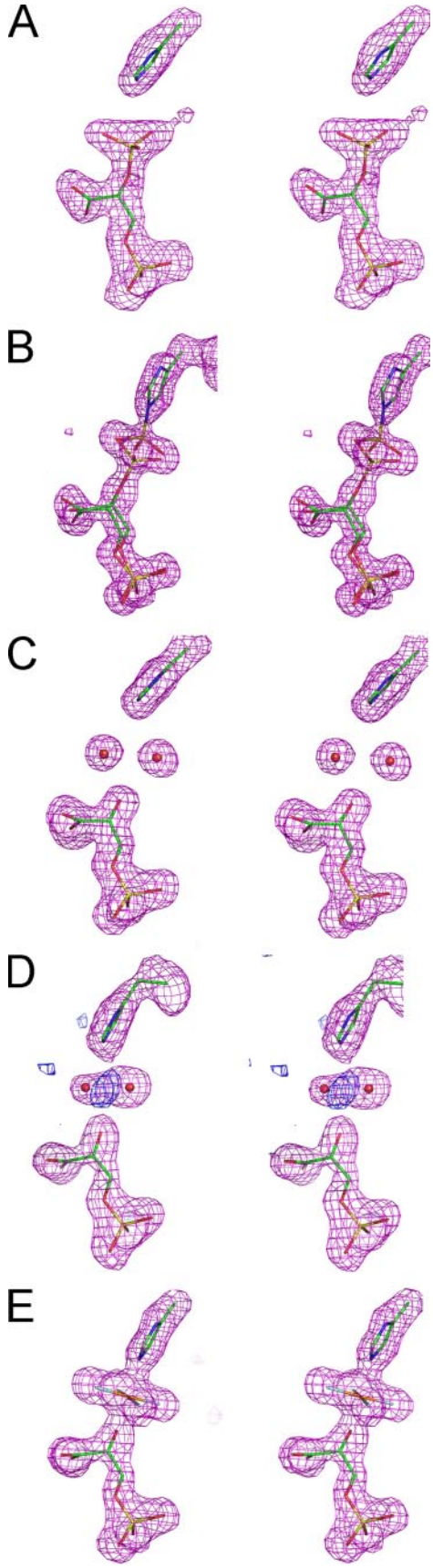

FIGURE 1. **A $F_o - F_c$ electron density map (contoured at 3.5 σ, *purple cage*) at the active site when the side chain of His-11 and the ligand are omitted.** *A* (*structure 1*), co-crystallized with 2,3-BPG at 4 °C. *B* (*structure 2*), co-crystallized with 2,3-BPG at 16 °C for less than 16 days. *C* (*structure 3*), only 3-PGA binding. *D* (*structure 4*), co-crystallized with 2,3-BPG at 16 °C for 17 days. Extra $F_o - F_c$ electron density (contoured at 3 σ, *blue cage*) exists when two water molecules and 3-PGA are modeled in. *E* (*structure 5*), co-crystallized with AlF_4^- and 3-PGA.

2,3-BPG by 0.5 Å. Consequently, the Nϵ-2 atom of His-11, central phosphorus atom, and the C-2 oxygen atom of 2,3-BPG are in a line, and the distance between the Nϵ-2 atom of His-11 to the C-2 oxygen atom is shortened from 5.1 to 4.6 Å (Fig. 5*A*). This conformation is consistent with an in line mechanism (1). To stabilize this conformation, Asn-17 moves its side chain toward the substrate, forming a hydrogen bond with the 2′-phosphoryl group. The side chain of Gln-28 also protrudes into the active site pocket, strengthening the hydrogen bond network.

Structure of BPGM Bound with 3-PGA—To further confirm the above equilibrated structures and to observe what would happen before and after the observed steps, BPGM crystals were grown with 2,3-BPG at room temperature (crystallization condition B) for different time periods, and the structures were determined. (Crystals suitable for diffraction could be obtained after growing for at least 12 days.) When crystals were allowed to grow for 12–16 days, the structures observed were similar to the equilibrated mixture described above. However, in crystals that were allowed to grow for more than 18 days, only 3-PGA was observed (Fig. 1*C*, *structure 3*). The 2′-phosphoryl group was absent, and His-11 was no longer phosphorylated. Two water molecules replaced the 2′-phosphoryl group (Fig. 5*E* and supplemental Fig. 2). This structure is quite stable and remains unchanged in crystals grown for 4 months. Consistent with the above observation, the 17th day crystal revealed that 2,3-BPG had almost converted to 3-PGA (Fig. 1*D*, *structure 4*). The backbone of residues 11–19 in structures 3 and 4 returned to a similar position as in structure 1, so that the imidazole ring of His-11 returned to the position it occupied at the start of the reaction. It suggests that this enzyme adopts a similar conformation at the beginning and the end of the reaction.

Structure of BPGM Bound with an Intermediate Analogue AlF_4^-—AlF_3 or AlF_4^- is often used to mimic the intermediate in phosphoryl transfer reactions. To investigate the intermediate structure, BPGM was crystallized from a solution containing 3-PGA, $AlCl_3$, and NaF (crystallization condition C). In this structure (Fig. 1*E*, *structure 5*), 3-PGA was observed to bind at the same position as above, and an AlF_4^- molecule was located between His-11 and 3-PGA with its AlF_4^- plane perpendicular to the line between the His-11 Nϵ-2 atom and the C-2 oxygen of 3-PGA (Figs. 1*E* and 5*F*; Supplemental Fig. 3). The enzyme conformation is almost identical to structure 2 with a root mean square deviation of 0.14 Å when all of the 250 Cα atoms are superimposed. The only significant structural difference is that His-11 shifts further toward 3-PGA by about 0.5 Å so that the distance from the His-11 Nϵ-2 atom to the 3-PGA C-2 oxygen atom is 4.1 Å. The aluminum atom is 2.1 Å from the Nϵ-2 atom of His-11 and 2.0 Å from the 3-PGA C-2 oxygen atom. The axial bond lengths are almost the same as in the pentavalent phosphorus intermediate of

β-phosphoglucomutase (28), although the structure of this intermediate is still a matter of argument (29, 30).

DISCUSSION

Our structures depict clearly the binding modes of 2,3-BPG and 3-PGA for the first time. In all of the BPGM complex structures we obtained, only the 2′-phosphoryl group was observed to access and donate the phosphoryl group to His-11, whereas the 3′-phosphoryl group remained distant (Fig. 4 and supplemental Figs. 1–3). Both 2′- and 3′-phosphoryl groups were tightly bound involving a number of hydrogen bonds. In addition, there was insufficient space for 2,3-BPG to rotate within the active site. Thus it is unlikely that both of the phosphoryl groups in 2,3-BPG could phosphorylate His-11, as proposed previously (3).

The above structures of the BPGM complex provide a series of snapshots of the process of phosphoryl transfer between 2,3-BPG and BPGM (Fig. 5*A*). These structures, for the first time, provide direct evidence that His-11 phosphorylation occurs by an in line partially associative mechanism. In the structure that mimics the transition state (Fig. 1*E*, *structure 5*), the distance between the nucleophile (His-11) and the leaving group is 4.1 Å, indicating the mechanism is 28% associative, approaching an S_N2 mechanism. The bond order here is similar to that observed in the pentavalent phosphorus intermediate of β-phosphoglucomutase (28).

In S_N2 nucleophilic substitution, stretching and then breaking of the bond to the leaving group occurred during the transformation of the reactants into the products. How could the distance between the nucleophile and the attacked atom be shortened? The motion of the catalytic His-11 offers the first glimpse. During the reaction, the backbone conformational changes of residues 11–19 drove the imidazole ring of His-11 to move back and forth, whereas 2,3-BPG and 3-PGA remained static with tight hydrogen binding (Fig. 5*B*). Besides, comparing BPGM structures 1 and 2 (Fig. 1, *A* and *B*), although both of them bind to 2,3-BPG, the conformations of the enzyme vary significantly. This indicates that the conformation of the enzyme in the substrate-bound state may differ from that in the reacting state. This is consistent with the idea that enzymes not only provide the reactive chemical group for catalysis but also, through conformational rearrangements, play a significant role in aligning the reactive atoms perfectly for the reaction (31).

In addition, comparison of the series of structures presented here shows the importance of His-188 and Glu-89 in catalyzing the phosphoryl transfer. Both these residues are

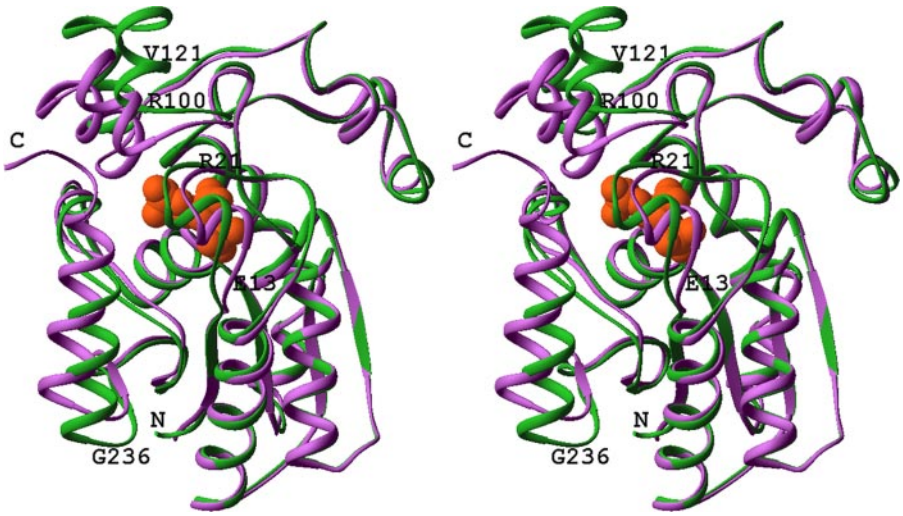

FIGURE 2. **Stereo drawing of the superposition of BPGM (*green*) and BPGM complexed with 2,3-BPG (*purple*).** 2,3-BPG is shown as *orange spheres*. The residues showing significant conformational changes and the N and C termini are *labeled*.

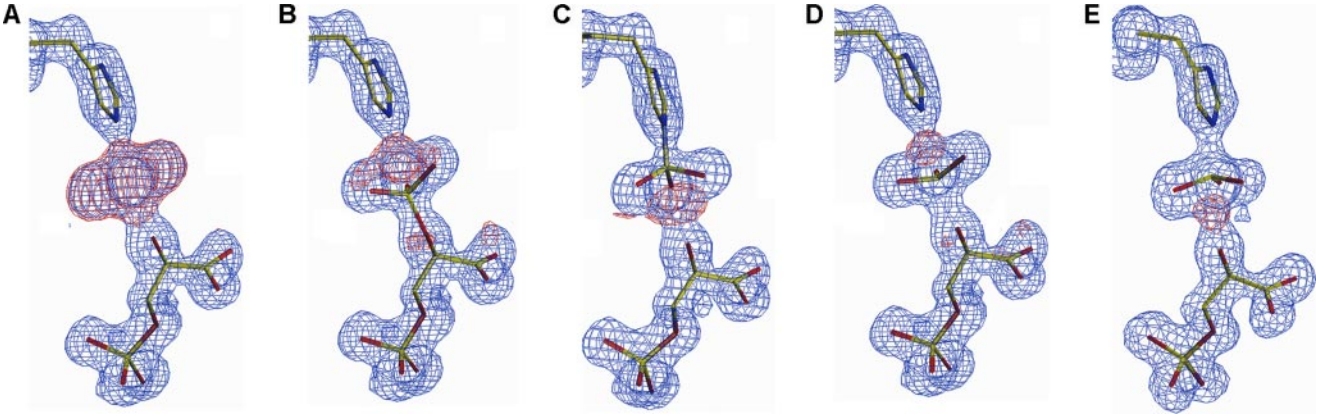

FIGURE 3. **Identification of the mixed ligands in the equilibrated structure (Fig. 1*B*, *structure 2*).** Ligands and the side chain of His-11 are shown with the omitted $F_o - F_c$ density map (*blue cages*) contoured at 3.5 σ. It is also shown with the extra F_o - F_c electron *density* (*red cages*, contoured at 3.5 σ) when different ligands were added in the model used for refinement. *A*, only 3-PGA was added. *B*, only 2,3-BPG was added. Extra electron density was located between His-11 and 2,3-BPG. *C*, a phosphoryl group covalent bond with the Nε-2 atom of His-11 to phosphorylate His-11 and 3-PGA was added. Extra electron density was located between 3-PGA and the phosphorylation group. *D* and *E*, the density was thought to be a 3-PGA plus a pentavalent phosphorus intermediate. The pentavalent phosphorus intermediate was finally refined at different locations in the two monomers. *D*, in monomer *A*. *E*, in monomer B. Some extra density still exists. Considering the instability of the pentavalent phosphorus intermediate, this possibility was ruled out.

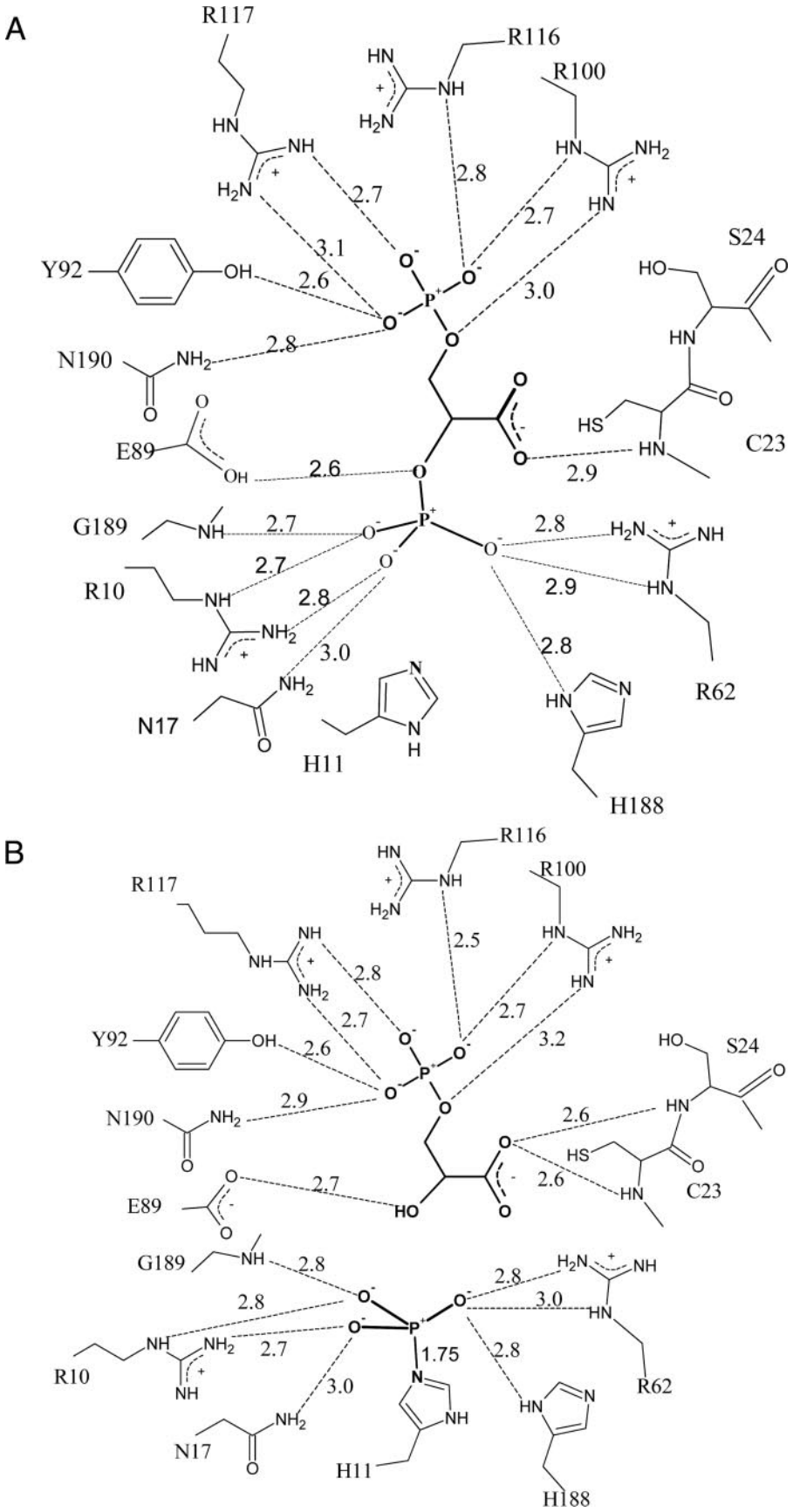

FIGURE 4. **Schematic of the interactions between the ligand and human BPGM with all interactions between the ligand and residues depicted as *dashed lines* and labeled with the bond lengths (Å).** *A*, interactions between 2,3-BPG and BPGM in the reacting state. *B*, interaction between 3-PGA and the phosphorylated enzyme.

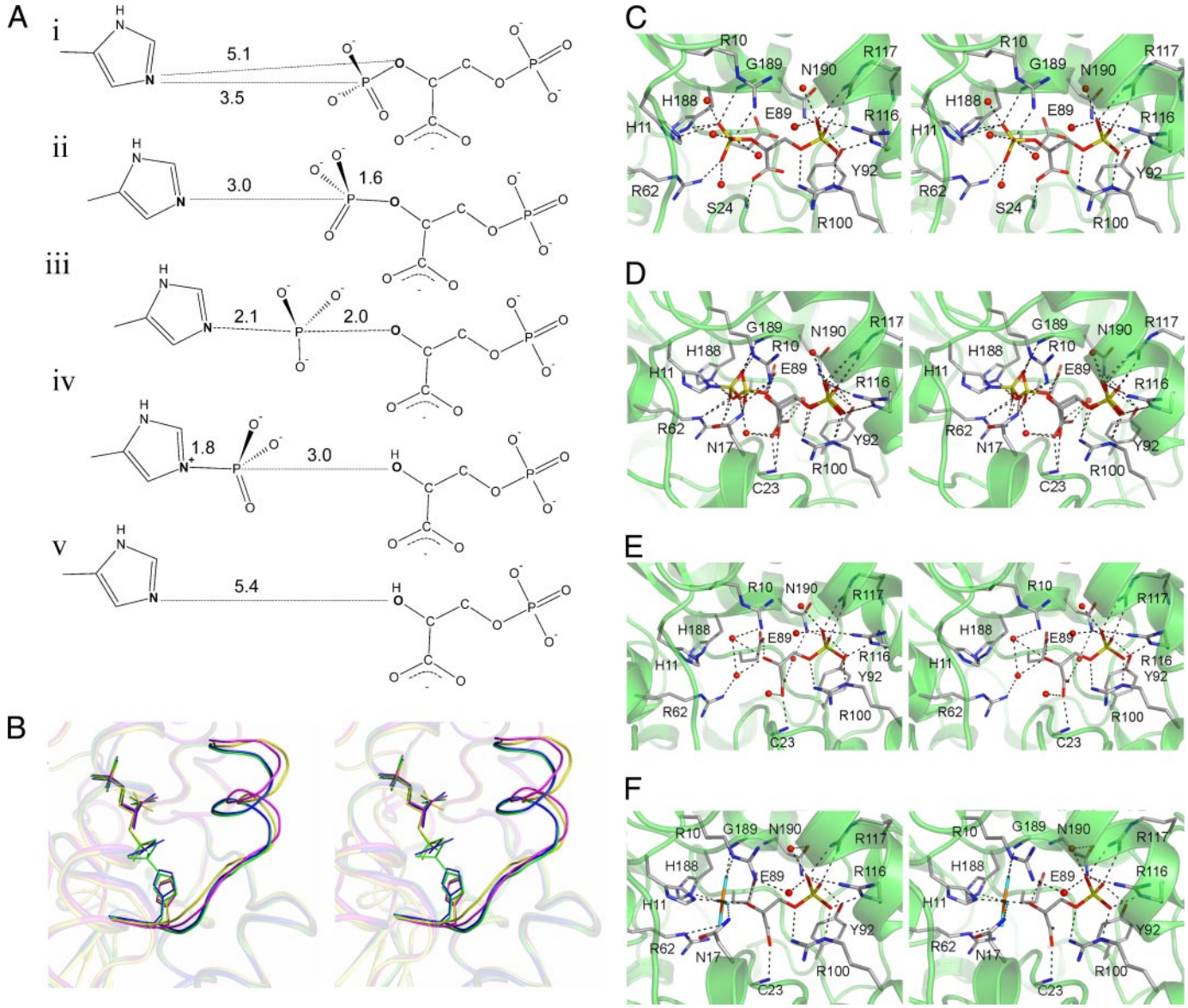

FIGURE 5. *A*, schematic of the distance (Å) variation between His-11 and the ligand during the phosphoryl transfer process. *i*, the binding state of 2,3-BPG. *ii*, the reacting state of 2,3-BPG. *iii*, the transition state derived from the structure with AlF_4^- and 3-PGA bound. *iv*, the phosphorylation state of His-11. *v*, binding with 3-PGA when the 2′-phosphoryl group is gone. *B*, stereo view of the motion of His-11 driven by the conformational changes of residues 11–21 during the reaction. The Cα root mean square deviation values for residues 11–21 between structures 1 and 2, structures 2 and 3 and structures 1 and 3 are 0.95, 1.10, and 0.48 Å, respectively; whereas in other regions, the root mean square deviation values are 0.23, 0.24, and 0.14 Å, respectively. Structure coloring: structure 1, *yellow*; structure 2, *green*; structure 3, *purple*; and structure 5, *blue*. *C*, *D*, *E*, and *F*, stereo views of the active sites of BPGM complexes. The critical residues in the active site pocket are *labeled*. The water molecules involved in ligand binding are represented by *red spheres*. *C*, structure 1. *D*, structure 2. *E*, structure 3. *F*, structure 5.

strictly conserved within the BPGM/dPGM family. His-188 hydrogen bonds to His-11, helping it to attain the correct position in free BPGM, and is involved in substrate binding in the complex. This explains why the mutation of His-188 to Ala in yeast dPGM results in a 1000-fold decrease in activity (32–34). On the other hand, Glu-89 is not directly involved in 2,3-BPG binding in structure 1 (Fig. 1*A*). However, during the reaction (the equilibrated structure), the carboxylate group of Glu-89 rotated about 90°, forming a hydrogen bond with the leaving group, the C-2 oxygen atom. This indicates that Glu-89 could act as a proton donor to the C-2 oxygen, helping the phosphoryl group to leave. This is consistent with the fact that the E89Q mutant has a slightly higher K_m value for 2,3-BPG but a k_{cat} value less than 5% of that of wild type (13).

Acknowledgments—We thank Drs. Peng Liu and Yuhui Dong of the Institute of High Energy Physics and Yi Han of the Institute of Biophysics for diffraction data collection. We also thank Dr. Sarah Perrett for critical reading and correction of the manuscript.

REFERENCES

1. Mildvan, A. S. (1997) *Proteins* **29,** 401–416
2. Lowe, G., Cullis, P. M., Jarvest, R. L., Potter, B. V., and Sproat, B. S. (1981) *Philos. Trans. R. Soc. Lond. B Biol. Sci.* **293,** 75–92
3. Fothergill-Gilmore, L. A., and Watson, H. C. (1989) *Adv. Enzymol. Relat. Areas Mol. Biol.* **62,** 227–313
4. Rose, Z. B. (1980) *Adv. Enzymol. Relat. Areas Mol. Biol.* **51,** 211–253
5. Rigden, D. J. (2003) *FEBS Lett.* **536,** 77–84
6. Walter, R. A., Nairn, J., Duncan, D., Price, N. C., Kelly, S. M., Rigden, D. J.,

and Fothergill-Gilmore, L. A. (1999) *Biochem. J.* **337,** 89–95
7. Winn, S. I., Watson, H. C., Harkins, R. N., and Fothergill, L. A. (1981) *Philos. Trans. R. Soc. Lond. B Biol. Sci.* **293,** 121–130
8. Wang, Y., Wei, Z., Bian, Q., Cheng, Z., Wan, M., Liu, L., and Gong, W. (2004) *J. Biol. Chem.* **279,** 39132–39138
9. Bond, C. S., White, M. F., and Hunter, W. N. (2002) *J. Mol. Biol.* **316,** 1071–1081
10. Bond, C. S., White, M. F., and Hunter, W. N. (2001) *J. Biol. Chem.* **276,** 3247–3253
11. Rigden, D. J., Alexeev, D., Phillips, S. E., and Fothergill-Gilmore, L. A. (1998) *J. Mol. Biol.* **276,** 449–459
12. Rigden, D. J., Walter, R. A., Phillips, S. E., and Fothergill-Gilmore, L. A. (1999) *J. Mol. Biol.* **286,** 1507–1517
13. Rigden, D. J., Walter, R. A., Phillips, S. E., and Fothergill-Gilmore, L. A. (1999) *J. Mol. Biol.* **289,** 691–699
14. Campbell, J. W., Watson, H. C., and Hodgson, G. I. (1974) *Nature* **250,** 301–303
15. Rigden, D. J., Mello, L. V., Setlow, P., and Jedrzejas, M. J. (2002) *J. Mol. Biol.* **315,** 1129–1143
16. Rigden, D. J., Littlejohn, J. E., Henderson, K., and Jedrzejas, M. J. (2003) *J. Mol. Biol.* **325,** 411–420
17. Wang, Y., Wei, Z., Liu, L., Cheng, Z., Lin, Y., Ji, F., and Gong, W. (2005) *Biochem. Biophys. Res. Commun.* **331,** 1207–1215
18. Muller, P., Sawaya, M. R., Pashkov, I., Chan, S., Nguyen, C., Wu, Y., Perry, L. J., and Eisenberg, D. (2005) *Acta Crystallogr. Sect D Biol. Crystallogr.* **61,** 309–315
19. Crowhurst, G. S., Dalby, A. R., Isupov, M. N., Campbell, J. W., and Littlechild, J. A. (1999) *Acta Crystallogr. Sect. D Biol. Crystallogr.* **55,** 1822–1826
20. Otwinowski, Z., and Minor, W. (1997) *Methods Enzymol.* **276,** 307–326
21. Brunger, A. T., Adams, P. D., Clore, G. M., DeLano, W. L., Gros, P., Grosse-Kunstleve, R. W., Jiang, J. S., Kuszewski, J., Nilges, M., Pannu, N. S., Read, R. J., Rice, L. M., Simonson, T., and Warren, G. L. (1998) *Acta Crystallogr. Sect. D Biol. Crystallogr.* **54,** 905–921
22. Jones, T. A., Zou, J. Y., Cowan, S. W., and Kjeldgaard. (1991) *Acta Crystallogr. Sect. A* **47,** 110–119
23. Laskowski, R. A., MacArthur, M. W., Moss, D. S., and Valenti, M. (1993) *J. of Appl. Crystallogr.* **26,** 283–291
24. Hayward, S., and Berendsen, H. J. (1998) *Proteins* **30,** 144–154
25. Theisen, M. J., Misra, I., Saadat, D., Campobasso, N., Miziorko, H. M., and Harrison, D. H. T. (2004) *Proc. Natl. Acad. Sci. U. S. A.* **101,** 16442–16447
26. Bahnson, B. J. (2004) *Proc. Natl. Acad. Sci. U. S. A.* **101,** 16399–16400
27. Van Wazer, J. R. (1964) *J. Dent. Res.* **43,** 1052–1064
28. Lahiri, S. D., Zhang, G. F., Dunaway-Mariano, D., and Allen, K. N. (2003) *Science* **299,** 2067–2071
29. Blackburn, G. M., Williams, N. H., Gamblin, S. J., and Smerdon, S. J. (2003) *Science* **301,** 1184
30. Webster, C. E. (2004) *J. Am. Chem. Soc.* **126,** 6840–6841
31. Wolf-Watz, M., Thai, V., Henzler-Wildman, K., Hadjipavlou, G., Eisenmesser, E. Z., and Kern, D. (2004) *Nat. Struct. Mol. Biol.* **11,** 945–949
32. White, M. F., and Fothergill-Gilmore, L. A. (1992) *Eur. J. Biochem.* **207,** 709–714
33. White, M. F., Fothergill-Gilmore, L. A., Kelly, S. M., and Price, N. C. (1993) *Biochem. J.* **291,** 479–483
34. Nairn, J., Price, N. C., Kelly, S. M., Rigden, D., Fothergill-Gilmore, L. A., and Krell, T. (1996) *Biochim. Biophys. Acta* **1296,** 69–75